STUDIA UBB CHEMIA, LXIV, 3, 2019 (p. 81-98)
(RECOMMENDED CITATION)
DOI:10.24193/subbchem.2019.3.07

THIN LAYER PHOTOCATALYSTS OF TiO_2-Ag COMPOSITES

BORBÁLA TEGZE[a], EMŐKE ALBERT[a], BOGLÁRKA DIKÓ[a], JÁNOS MADARÁSZ[b], GYÖRGY SÁFRÁN[c], ZOLTÁN HÓRVÖLGYI[a,*]

ABSTRACT. Mesoporous TiO_2 coatings were prepared by sol-gel dip-coating method on glass and SiO_2 coated glass substrates. They were modified with silver by two different methods: impregnation of as-prepared coatings in $AgNO_3$ aqueous solution; coating deposition from precursor sols containing $AgNO_3$. Transmittance spectra, refractive index, layer thickness and porosity were determined by UV-Vis spectroscopy. Crystallinity of the samples was characterized by XRD, and the morphology and structure by HR-TEM. Photoinduced wettability conversion of the samples was studied, and it was found that the presence of the SiO_2 barrier layer and the silver content had significant effect on the wetting behaviour. The photoactivity and reusability of the samples were investigated with methyl orange dye degradation under ultra-violet (UV) irradiation. TiO_2 coatings impregnated in 1M $AgNO_3$ solution were found to be the most stable photocatalyst system.

Keywords: *TiO_2, photocatalysis, self-cleaning, dye degradation, sol-gel coatings*

INTRODUCTION

Titania is a highly effective photoactive material, with great promise in the fields of photocatalysts, solar cells, *etc.*[1–5] For many applications it can be a great advantage to use TiO_2 in coating form: *e.g.* in air- and water purification via photocatalytic means, coatings offer easier separation of the photocatalyst from the polluted fluid and a more manageable system compared

[a] *Budapest University of Technology and Economics, Faculty of Chemical Technology and Biotechnology, Department of Physical Chemistry and Materials Science, Centre for Colloid Chemistry, H-1521 Budapest, Budafoki út 6-8, Hungary*
[b] *Budapest University of Technology and Economics, Faculty of Chemical Technology and Biotechnology, Department of Inorganic and Analytical Chemistry, Technical Analytical Chemistry Research Group, H-1521 Budapest, Szent Gellért tér 4, Hungary*
[c] *Centre for Energy Research, Institute for Technical Physics and Materials Science, H-1121, Budapest, Hungary*
** Corresponding author: zhorvolgyi@mail.bme.hu*

to other forms (*i.e.* powders).[6] TiO_2 films on solid substrates, such as glass, are a promising type of self-cleaning coating, used for *e.g.* windows, solar panel coverages.[7] Photoinduced wettability conversion is another commonly observed property of TiO_2: under UV light the surface becomes more hydrophilic, and this change in wettability is reversible. This behaviour has practical importance for several applications, especially for anti-fogging and self-cleaning coatings. The most accepted explanation for this phenomenon is that photogenerated holes in TiO_2 can react with lattice oxygen, which leads to the formation of surface defect sites (oxygen vacancies). Water molecules from the atmosphere dissociatively adsorb on these defect sites and form hydroxyl groups, causing increased hydrophilicity. Following the UV treatment, if the samples are kept in dark, under visible light or at a higher temperature, the surface gradually becomes more hydrophobic once again, as oxygen adsorption replaces the adsorbed water and “heals” the defect sites. [8–10]

An important aim of researchers is to increase the photoactivity of TiO_2 coatings: one known way to achieve this is through modification with noble metals, one of the most suitable options is silver.[11,12] Furthermore, silver particles on the surface provide antibacterial properties [13–15], which is also an attractive function for many practical uses. There are several reasons for the increased photoactivity of titania-silver composite coatings. The main reason is that silver particles can increase the time of the photo-induced charge separation of electrons and holes (silver particles act as electron traps by forming a Schottky barrier at the semiconductor-metal interface) [16]. In certain cases, surface plasmon resonance of silver nanoparticles [17], and band-gap narrowing of the photocatalyst [18] was observed, which can contribute to a wider wavelength range of solar light being utilized.

TiO_2 coatings can be prepared by a variety of methods. The sol-gel technique can produce thin coatings of high surface area with a mesoporous system, which provides possibilities of easy control of structure, composition and layer thickness [19]. There are different methods for the preparation of titania-silver sol-gel composite coatings: the most often used is simply adding silver-compound (e.g. $AgNO_3$) to the precursor sol [20–22]. The impregnation method is used less often: the advantage is that a greatly decreased amount of silver is needed, while the ordered pore structure of the coatings remains unchanged; the disadvantage is that this method needs an additional step during the preparation. In the impregnation method the coating is immersed in $AgNO_3$ solution, dried and then a post-treatment is carried out to reduce the silver ions, *e.g.* UV irradiation [23,24] or heat treatment [25]. The comparison of these different silver modification methods, and studying how the amount, location and other parameters of the silver particles present in the coatings influences the photoactivity and the stability of these photocatalysts can have relevance for future research and applications.

In this paper mesoporous titania sol-gel coatings on glass substrate are prepared and modified with silver by the impregnation method, using two different concentrations of $AgNO_3$ solution. For comparison, porous titania-silver composite coatings are also prepared by the more often used method of adding silver to the precursor solution. Compact SiO_2 barrier layer was deposited on the glass substrate, in order to inhibit ion diffusion (mainly Na^+) from the glass to the titania layer, which is known to decrease its photoactivity [26]. The coatings are characterized by UV-Vis spectroscopy, X-ray diffraction, transmission electron microscopy and wettability measurements, including the investigation of photoinduced wettability conversion. The photoactivity of the samples is studied with dye degradation under UV light, including repeated measurements, to evaluate the stability and reusability of the photocatalytic samples. The effectiveness of the SiO_2 barrier layer is also investigated. The results were analysed with the aim of discovering the connections between the parameters of the silver modification and the structure, photoactivity and photocatalytic stability of the titania coatings, in order to develop cost effective photocatalyst systems with highly increased photoactivity and good stability.

RESULTS AND DISCUSSION

The transmittance spectra of the prepared titania samples can be seen in Fig. 1a. SiO_2 coatings improve the light transmittance of the glass substrate, due to their lower refractive index, while TiO_2 – both as a first and as a second layer - causes a decrease in transmittance, since its refractive index is higher. Silver modification of the SiO_2/TiO_2 coatings by impregnation in $AgNO_3$ solution resulted in lowered light transmittance, due to the presence of silver particles: this change was minimal in the case of TiO_2-Ag(0.03M) samples, while more noticeable in the case of TiO_2-Ag(1M) coatings. This indicates that with higher $AgNO_3$ impregnating solution concentration a higher Ag content could be reached in the coatings. The TiO_2/Ag coatings, which were prepared by adding $AgNO_3$ directly to the precursor sol, had the lowest transmittance of all samples, as a result of their high Ag content. The absorbance spectra of the different silver modified coatings can be seen in Fig. 1b. Comparing the different silver modification methods, only a slight absorbance increase could be observed as a result of the impregnation in $AgNO_3$, while the TiO_2/Ag coatings showed significantly higher absorption. This difference could also be observed in the colour of the samples: TiO_2-Ag coatings were almost completely transparent, while TiO_2/Ag coatings showed a deeper grey colour. The TiO_2/Ag samples also show a peak around 506 nm, which can be attributed to the surface plasmon absorption of Ag particles [27]. The effective

refractive index (n), layer thickness (d) and porosity (P) values of the coatings determined from the transmittance data can be seen in Table 1. The titania coatings had a layer thickness around 100 nm, and a porosity of 32-37%. The titania layer thickness of the $SiO_2/TiO_2/Ag$ samples was estimated to be 116 nm, from the optical analysis of coatings that were prepared the same way, with the exception that no $AgNO_3$ was added to the precursor sol. The presence of the SiO_2 barrier layer caused a slight change in the properties of the TiO_2 coatings, with a small increase in refractive index and decrease in thickness values. The one-sided coatings made for the photocatalysis tests showed almost completely identical properties to the conventionally prepared two-sided coatings, thus, the experiments carried out on these two types of samples can be readily compared.

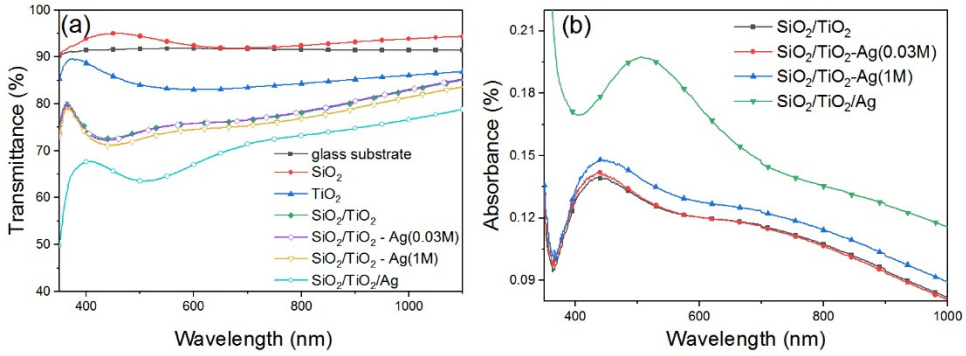

Figure 1. Transmittance (a) and absorbance (b) spectra of the coatings (two-sided samples)

Table 1. Effective refractive index (n), layer thickness (d) and porosity (P) values of the coatings

Sample type	n (-)	d (nm)	P (%)
SiO_2	1.447 ± 0.003	228 ± 23	-
TiO_2 on glass	1.696 ± 0.024	113 ± 2	37 ± 2
TiO_2 on SiO_2 coated glass	1.761 ± 0.016	83 ± 6	33 ± 1
SiO_2 (one-sided)	1.456 ± 0.002	226 ± 3	-
TiO_2 on SiO_2 coated glass (one-sided)	1.767 ± 0.030	87 ± 2	32 ± 1

The theoretical silver content of the TiO_2/Ag coatings calculated from the precursor sol composition is 11.8 wt%. During the calculation of the silver content of TiO_2-Ag coatings, it was assumed that the $AgNO_3$ impregnating solution completely filled the pore volume: silver content was estimated as 0.0421 wt% and 1.38 wt% for TiO_2-Ag(0.03M) and TiO_2-Ag(1M) samples, respectively. These estimated values can be compared with previous Rutherford backscattering spectroscopy measurements of TiO_2-Ag(1M) and TiO_2-Ag(0.03M) coatings prepared on silicon wafers, as reported in our paper [14]: the silver content was found to be 1.07 wt% for TiO_2-Ag(0.03M) samples and 2.37 wt% for TiO_2-Ag(1M) samples. The silver content increased with increasing concentration of $AgNO_3$ impregnating solution, although this increase was not linear. The theoretically calculated values are significantly lower than the measured silver content, suggesting strong adsorption of silver ions on the titania surface. The TiO_2/Ag coatings are estimated to have a silver content of one order of magnitude higher (~12 wt%) compared to the other silver modification method (1-2 wt%).

XRD measurements were first carried out on TiO_2 coatings on SiO_2 coated glass substrates. However, only a low intensity peak around $2\Theta = 25°$ (suggesting anatase crystal phase) could be seen on the XRD pattern (not shown). This weak signal was due to the very low layer thickness of the titania coatings. In order to get better XRD results, TiO_2 powder was prepared from the same precursor sol as used in the coating deposition, and different heat treatments were applied. Three types of silver modified TiO_2 samples were prepared to model the three types of coatings: TiO_2 powder was impregnated in 0.03 M and 1 M $AgNO_3$ solutions; while a TiO_2/Ag powder sample was also prepared from the precursor sol that contained $AgNO_3$. The XRD pattern of these powder samples showed well-defined and multiple peaks, as seen in Fig. 2. The average crystallite sizes and the phase content of the crystalline parts were determined from the XRD pattern, and can be seen in Table 2. TiO_2 powder sample heat-treated at 450 °C (the same as applied during coating preparation) was found to be of mainly anatase phase, with a very small amount of rutile phase. The same TiO_2 sample, when heat-treated at 600 °C, showed narrower, more separated peaks at its XRD pattern, suggesting that higher crystallinity was reached at this higher temperature. This was further confirmed by comparing the calculated crystallite sizes, as seen in Table 2. The composition of the crystalline phases was found to be the same (93 wt% anatase, 7 wt% rutile). No rutile phase was found in the TiO_2/Ag sample (100 wt% anatase), its XRD pattern indicated higher amorphous content compared to the other samples, and the average crystallite size was also estimated to be slightly lower. This difference is most likely due to the different precursor sol composition used for the preparation of these samples.

In comparison, the TiO_2-Ag(0.03M) and TiO_2-Ag(1M) powder samples also contained rutile phase in a small, but slightly higher amount (11 wt% rutile), and slightly higher average crystallite sizes were determined compared to the TiO_2 sample heat treated at the same temperature. The increase of both the crystallite size and the rutile phase content in these Ag modified samples can be a result of the much longer time spent at high temperature, as two consecutive heat treatments were applied during their preparation. However, it's still unexpected that these samples have higher rutile content than the TiO_2 sample treated at 600 °C, since anatase crystal phase transforms into rutile at 500-800 °C [28]. Another possibility is that the higher rutile content was due to the $AgNO_3$ decomposition during the heat treatment: the heat from this exothermic reaction can facilitate the anatase-rutile transformation [29]. Thus, the additional step needed in this silver modification method, which can be seen as a disadvantage, can also cause beneficial effects: the second heat treatment caused increased crystallinity and rutile phase content. Both of these can contribute to higher photocatalytic activity, since it was found in several studies that mainly anatase crystal phase with a low rutile content is a more effective system compared to pure anatase [2].

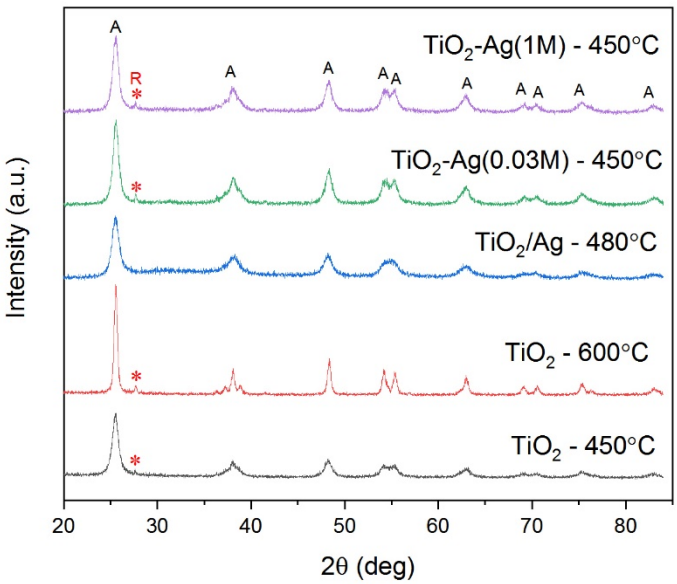

Figure 2. XRD pattern of TiO_2 powder samples (A: anatase, R: rutile)

Table 2. Average crystallite sizes and phase content of crystalline parts determined from the XRD pattern

Sample type	crystallite size	anatase wt%	rutile wt%
TiO_2 (450 °C)	11.8 nm	93	7
TiO_2 (600 °C)	20.2 nm	93	7
TiO_2/Ag (480 °C)	10.6 nm	100	-
TiO_2-Ag(0.03M) (450 °C)	12.7 nm	89	11
TiO_2-Ag(1M) (450 °C)	12.4 nm	89	11

Fig. 3. shows the cross-sectional TEM (a, b), HR-TEM (c) and EELS (d) images of TiO_2 (a) and TiO_2-Ag(1M) (b, c, d) coatings on Si substrates. The porous structure is visible and similar for both samples, and the layer thickness determined from the images (Fig. 3a-b) is the same for both coatings (72 nm, which is in good agreement with the value determined by optical analysis). Hence, the silver modification of the samples did not damage their initial pore system. The coatings are made of interconnected TiO_2 particles that form a pore system that is irregularly structured, but largely homogeneous throughout the coating. According to high resolution TEM (Fig. 3c), the coating consists of 6-11 nm sized crystalline (anatase) TiO_2 particles. The dark particle seen on the surface of the coating in this image is likely a silver metal particle. This can be confirmed by the EELS plasmon image of the TiO_2-Ag(1M) sample (Fig. 3d): the Ag particles appear as dark contrast features, while the oxide matrix exhibits bright contrast (the darker contrast is attributed to metallic behaviour). The sample contains clearly visible, relatively large Ag particles of 6-14 nm on the surface and also within the pores of the layer. It's suggested that in addition to the large particles there are also much smaller ones, inside the pores, which are too small to be detected.

Wettability of TiO_2 coatings and the photoinduced changes in this property were studied by measuring water contact angles. Advancing (Θ_A), receding (Θ_R) and Young's contact angles (Θ_{Young}), and contact angle hysteresis (H) values of the different samples on SiO_2 coated glass can be seen in Table 3. The as-prepared coatings were found to be hydrophilic, with a high contact angle hysteresis (15-20°). After 5 min UV irradiation, all samples showed complete wetting (contact angle 0°). After storing these samples in dark for several days, the contact angle values increased and reached values significantly above their initial value (by about 30°, see Table 3), and after various treatments (e.g. UV and Vis irradiation cycles) the lower original values that could be measured on the as-prepared samples were not recovered, most

likely due to photocorrosion processes. Generally, all samples on SiO_2 coated glass after longer Vis irradiation and/or storage in darkness showed advancing contact angle values between 45° and 80°. Samples modified by $AgNO_3$ solution impregnation showed similar contact angles to that of the pure TiO_2 coatings. In contrast, the TiO_2/Ag samples made from $AgNO_3$ containing precursor sol showed significantly lower contact angles. This can be explained by the differences in coating structure caused by the presence of $AgNO_3$ in the precursor sol; while it is also possible that this silver modification method resulted in a significant amount of highly dispersed, small Ag particles present on the surface, capable of fast silver ion diffusion into water, which caused higher polarity and hydrophilicity.

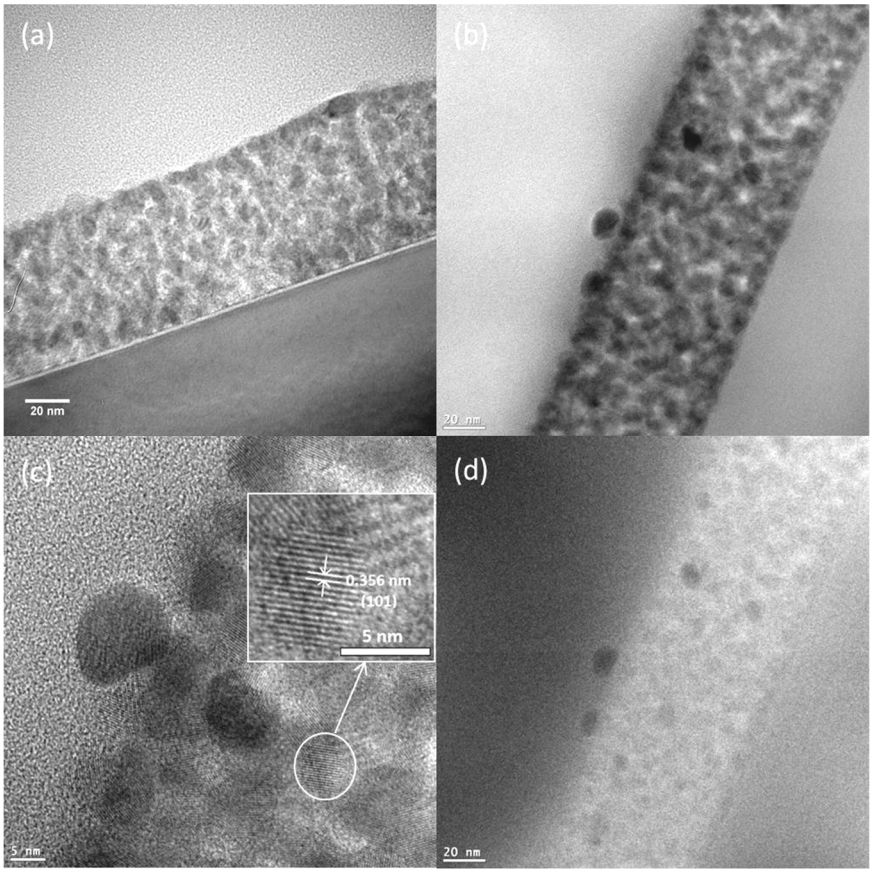

Figure 3. Cross-sectional TEM images of TiO_2 (a) and TiO_2-Ag(1M) (b) coatings; HR-TEM image (c) and EELS plasmon image (d) of the same TiO_2-Ag(1M) sample.

Table 3. Advancing (Θ_A), receding (Θ_R) and Young's contact angles (Θ_{Young}) and contact angle hysteresis (H) values of samples made on SiO_2 coated glass, measured right after preparation and after 5 min UV irradiation followed by 2 days in dark

	Θ_A (°)	Θ_R (°)	Θ_{Young} (°)	H (°)
	as-prepared			
TiO_2	31 ± 4	16 ± 3	24 ± 3	15 ± 1
TiO_2-Ag(0.03M)	31 ± 6	14 ± 5	24 ± 5	17 ± 4
TiO_2-Ag(1M)	37 ± 5	18 ± 5	29 ± 4	20 ± 4
TiO_2/Ag	12 ± 2	-	-	-
	5 min UV, 2 days in dark			
TiO_2	57 ± 8	34 ± 6	47 ± 7	23 ± 3
TiO_2-Ag(0.03M)	68 ± 10	43 ± 6	56 ± 8	25 ± 3
TiO_2-Ag(1M)	73 ± 7	48 ± 6	61 ± 6	25 ± 2
TiO_2/Ag	45 ± 9	30 ± 8	38 ± 8	15 ± 2

The TiO_2 coatings prepared on bare glass were found to be even more hydrophilic: all types of samples on bare glass showed complete wetting, even after 2 days of storage in dark (seen also in Fig. 4). This considerable difference between the same coating types prepared on different surfaces is due to the Na^+ migration from the glass into the titania layer during the heat treatment of the coating preparation, which is only possible in the absence of SiO_2 barrier layer. The high Na^+ content of TiO_2 samples on bare glass causes higher polarity and increased hydrophilicity. The Na ions can diffuse into the water droplets placed on the sample, further increasing the surface polarity.

Several cycles of UV irradiation/regeneration under visible light were repeated on the samples. The comparison of TiO_2 and $AgNO_3$ solution impregnated TiO_2 samples can be seen in Fig. 4. All samples showed photoinduced wettability conversion behaviour through multiple cycles. However, this effect was much smaller in the case of the coatings prepared on bare glass substrates, most likely due to their high Na^+ content. Slower regeneration of hydrophobicity was observed with increasing Ag content. Presumably, the Ag particles present in the samples can form silver ions, and may even diffuse into the water placed on the surface during the contact angle measurements, leading to a more hydrophilic surface when compared to pure TiO_2.

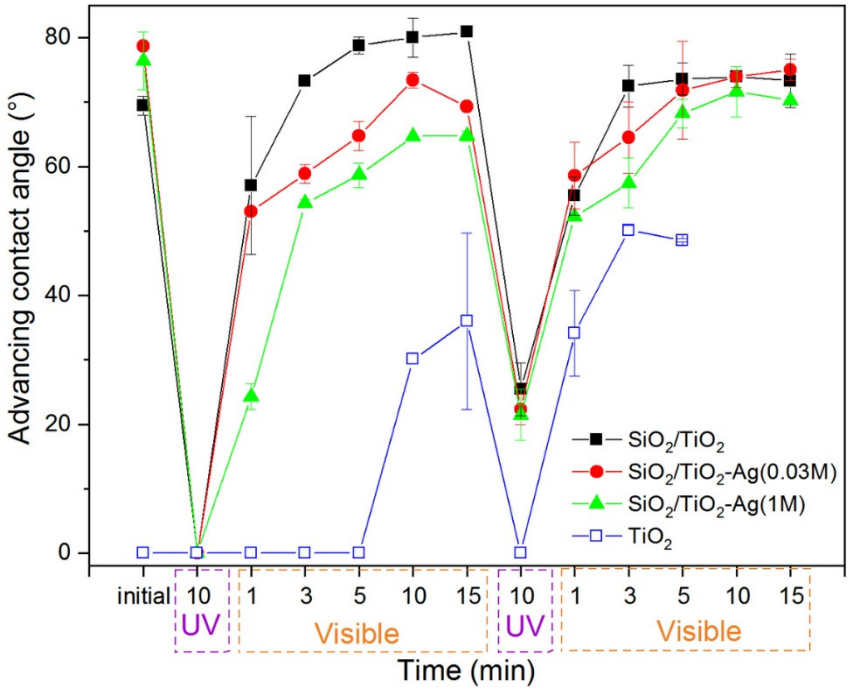

Figure 4. Advancing contact angles measured on TiO_2 and TiO_2-Ag samples during two UV/Vis cycles

Photoactivity of the samples was studied using methyl orange dye solution. In the first tests, the photocatalytic activity of TiO_2, TiO_2-Ag(0.03M) and TiO_2-Ag(1M) samples was compared. Fig. 5a shows the absorbance decrease of the dye solution during UV irradiation, on the example of a TiO_2 coating prepared on SiO_2 coated glass. A peak attributed to methyl orange can be seen at 465 nm [30]. Dye decolourization was compared for different samples by determining A/A_0, where A is the absorbance at 465 nm after t time of UV irradiation, and A_0 is the initial absorbance at 465 nm before irradiation (Fig. 5b). All TiO_2 samples on SiO_2 coated glass showed significant photoactivity. In comparison, the photoactivity of samples prepared on bare glass was found to be drastically decreased due to their high Na^+ content, dye degradation was minimal. Dye photodegradation was found to follow pseudo-first order reaction.The degradation rate constants (k) were determined by linearization of the measured $A/A_0 - t$ values, using the following equation:

$\ln(A/A_0) = -kt$. The k value was determined from the slope of the line fitted to the data points. The degradation rate constants were 0.12 ± 0.04 h^{-1} for SiO_2/TiO_2, 0.30 ± 0.04 h^{-1} for SiO_2/TiO_2-Ag(0.03M), 0.33 ± 0.08 h^{-1} for SiO_2/TiO_2-Ag(1M), and 0.35 ± 0.04 h^{-1} for SiO_2/TiO_2/Ag samples. These results show that the dye photodegradation was significantly faster in the silver modified coatings compared to the pure titania coatings. The silver content of the samples did not appear to influence the photoactivity: lower Ag content was enough to achieve a high photoactivity increase. However, another important question is the stability and reusability of these photoactive coatings: whether the samples can degrade the dyes in repeated tests with the same efficiency, or if over time their photoactivity would decrease. Furthermore, in our previous paper [14], it was found that the silver content of similarly prepared samples decreases in time while they are immersed in an aqueous solution – it's likely that this process can influence the photoactivity of the coatings. For this reason, the samples were further evaluated in repeated photocatalysis tests.

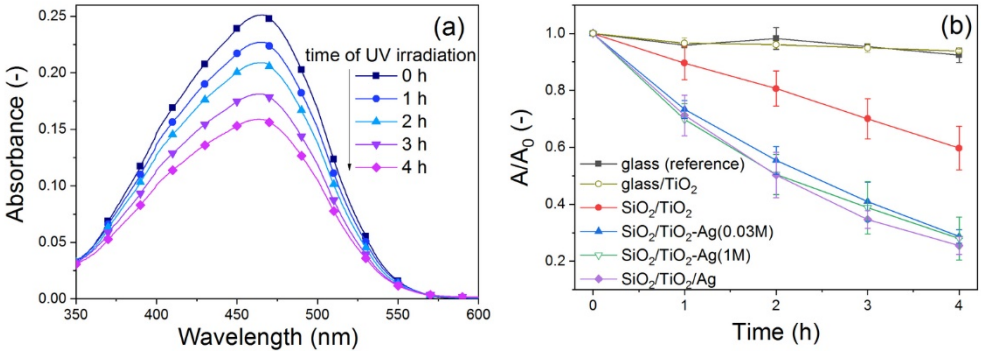

Figure 5. Photocatalysis measurements: (a) absorbance decrease of methyl orange solution containing SiO_2/TiO_2 sample under UV light; (b) A/A_0 – t curves of different samples

In these repeated measurements, the samples were irradiated for 4 × 4 h: after each 4 h irradiation a new dye solution was used for the same sample. The decrease in concentration of dye molecules was estimated by the A/A_0 value after each 4 h UV irradiation, and the dye degradation efficiency (D) of the different samples was calculated by the following equation: $D = (1\text{-}A/A_0) \times 100\%/a$, where a is the area of the coating sample.

In order to have a well determined area of coating in contact with the dye solution, coatings were deposited on only one side of the glass substrate using a special sample holder during the dip-coating process. All titania coatings were prepared on SiO_2 coated glass for these measurement.

As it can be seen in Fig. 6, the pure titania coatings showed a stable photoactivity during the full 16 h irradiation of the photocatalysis tests. Similarly, to the previously described experiments, the results of the repeated tests showed that all Ag modified coatings showed significantly increased dye degradation compared to the pure TiO_2 samples. It was found that dye degradation efficiency values (determined after the first 4 h of irradiation) did not increase with increasing the amount of silver in the samples. However, it was found that even though the TiO_2-Ag(0.03M) samples initially had the highest photoactivity, this photoactivity decreased after the test was repeated several times. In contrast, the TiO_2-Ag(1M) samples, which contained a higher amount of silver particles, did not show significant photoactivity decrease during the measured time interval (16 hours). It can be assumed that the silver particles on the titania surface start to dissolve and diffuse as silver ions into the aqueous solution during the measurement [14]. After a certain time, enough silver is removed from the coating that the photoactivity starts to decrease. While initially a lower surface coverage of silver might even be advantageous, during repeated use the photoactivity decrease would occur much slower in the impregnated samples with the higher Ag content. This is why TiO_2-Ag(0.03M) samples showed higher initial photoactivity, but TiO_2-Ag(1M) samples kept their high photoactivity for longer during repeated use. The speed of this process can also depend on the sizes and dispersity degree of the silver particles, and in this, there might also be differences between the samples. It's possible that bigger Ag particles could form in the TiO_2-Ag(1M) coatings due to the much higher $AgNO_3$ impregnating solution concentration used, which would also cause slower dissolution. Interestingly, the TiO_2/Ag coatings that contained the highest amount of silver also showed a slight decrease in photoactivity. Possibly the reason for this is that in the TiO_2/Ag coatings only some amount of the Ag particles are on the surface and accessible during the photocatalytic degradation, and silver is also incorporated into the TiO_2 matrix; while with the impregnated TiO_2-Ag coatings the accessibility of the silver particles is ensured. In these experiments, the silver particles present on the surface (or in the vicinity of the surface) seemed to play a more significant role in the rate of dye photodegradation, than the silver present in the matrix.

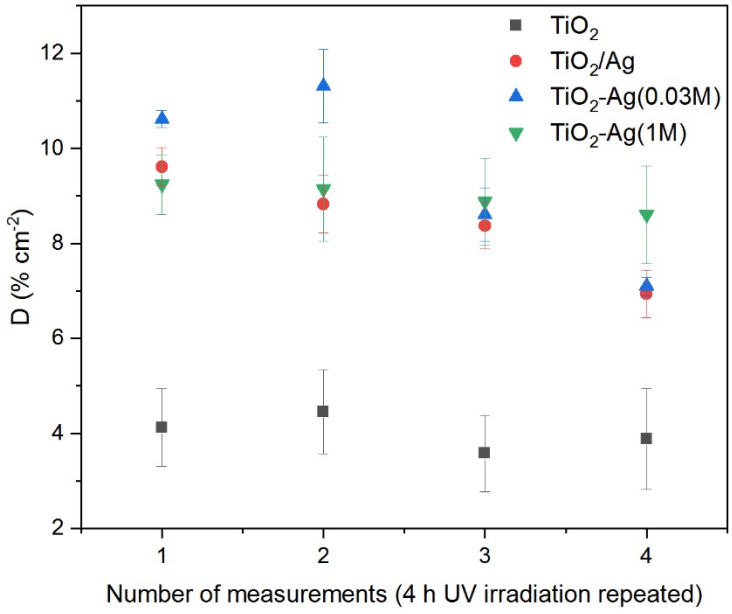

Figure 6. Repeated photocatalysis measurements

CONCLUSIONS

The results show that the method and parameters of silver modification have an important impact on the long-term photocatalytic activity of titania coatings. Silver modification via impregnation in $AgNO_3$ solution followed by a heat treatment is a promising method for increasing the photoactivity of self-cleaning TiO_2 coatings. The second heat treatment, which was carried out in order to reduce silver ions, was found to have further beneficial results: the crystallinity increased, and rutile-anatase mixed crystal phase was achieved, which can both improve photoactivity. The prepared titania coatings had a highly porous, crystalline structure. SiO_2 barrier layer was applied on the glass substrates, which led to improved photocatalytic properties and more pronounced photoinduced wettability conversion behaviour, both important for practical applications. Complete wetting was achieved under UV light, which means that water and aqueous media can penetrate the pores, and the high surface area provided by the porous structure can be fully utilized. The reusability and stability of the photocatalyst layer can be ensured by choosing an optimal silver content, which can be controlled by impregnation parameters (*e.g.* concentration of impregnating $AgNO_3$ solution).

EXPERIMENTAL SECTION

All reagents were analytical grade and used without further purification. The following materials were used for the preparation of the samples: hexadecyltrimethylammonium bromide (CTAB, 99+%, Acros Organics), Pluronic P123 (P123, average mol wt 40000, Sigma Aldrich), hydrochloric acid (HCl, 37%, Reanal), nitric acid (HNO_3, 65%, Lach-Ner), tetraethyl orthosilicate (TEOS, 99%, Merck), titanium (IV) butoxide (98%, Merck), titanium (IV) isopropoxide (98+%, Acros Organics), acetylacetone (99+%, Acros Organics), $AgNO_3$ (99.8%, Lach-Ner), 2-propanol (99+%, Acros Organics), ethanol (EtOH, 99.7+%, Reanal), purified distilled water (filtered with Millipore Simplicity 185 system to reach 18.2 MΩ cm). Methyl orange dye (95%, Acros Organics) was used in the photocatalysis tests.

Preparation of coatings

TiO_2 and two-layered SiO_2/TiO_2 coatings were prepared on glass substrates using sol-gel dip-coating. Silver modified TiO_2 samples were prepared by two methods: by adding $AgNO_3$ to the precursor sol, and by impregnation of as-prepared TiO_2 samples in $AgNO_3$ solutions followed by heat treatment. Some titania samples were also deposited on silicon wafers for the HR-TEM measurements. For the photocatalysis tests one-sided samples were prepared using a laboratory made sample holder that covered one side of the substrate. The synthesis of precursor sols via acid catalysed hydrolysis and polycondensation of silicon- and titanium-alkoxides was similar to that reported previously [14,31]. Compact SiO_2 barrier layers were prepared from precursor sols with molar ratios of TEOS : EtOH : HCl : H_2O - 1 : 4.75 : 7.2×10^{-4} : 4.00. For the porous TiO_2 coating preparation the molar ratios of titanium (IV) butoxide : EtOH : HNO_3 : H_2O : CTAB were 1 : 27.74 : 0.39 : 1.54 : 0.124 in the precursor sol. Porous TiO_2/Ag composite coatings were also prepared from precursor sols that contained $AgNO_3$, with molar ratios of titanium (IV) isopropoxide : EtOH : acetylacetone : H_2O : P123 : $AgNO_3$ - 1 : 33.80 : 0.97 : 2.19 : 0.034 : 0.1. Film deposition from the precursor sols onto clean glass and Si substrates (cleaned with 2-PrOH and distilled water) and SiO_2 coated glass substrates was carried out with a dip-coater (Plósz Mérnökiroda Kft., Hungary) using withdrawal speeds of 6 cm min^{-1} for SiO_2 barrier layers, and 12 cm min^{-1} for TiO_2 coatings. As the thickness of the coatings can be controlled by the withdrawal speed, these values were selected in order to prepare continuous, homogeneous and transparent films of desired layer thicknesses, with good repeatability. Samples were placed in an oven (Nabertherm B170) for heat treatment at 480 °C for 1 h (TiO_2/Ag

coatings), or 450 °C for 30 min (all other samples). The heat treatment parameters were chosen to reach suitable stability and avoid significant shrinkage of the coatings. To prepare two-layered SiO_2/TiO_2 coatings, the SiO_2 layer was dip-coated followed by a heat-treatment, and these steps were then repeated with the appropriate parameters to prepare the second, titania layer. Silver modified titania coatings denoted as TiO_2-Ag(0.03M) and TiO_2-Ag(1M) samples were prepared by impregnation of porous TiO_2 samples in $AgNO_3$ aqueous solutions of 0.03 M or 1 M concentrations. The impregnation was carried out with the dip-coater using a dipping speed of 1 cm min^{-1} and withdrawal speed of 10 cm min^{-1}. The samples were then washed with distilled water, dried, and placed in an oven for heat-treatment at 60 °C for 30 min, then 450 °C for 30 min.

Measurements and methods

The transmittance spectra of the glass substrates and the coated samples were measured by an Analytic Jena Specord 200–0318 UV-Vis spectrophotometer, in the wavelength range of 350-1100 nm, using air as reference, a scanning speed of 10 nm s^{-1} and a resolution of 1 nm. The refractive index (at 632.8 nm) and layer thickness values of SiO_2, TiO_2 and SiO_2/TiO_2 two-layered coatings on glass substrates were calculated from the transmittance spectra using thin layer optical models [32]. The porosity of these coatings was estimated from the measured effective refractive index using the Lorentz-Lorenz formula [33].

The crystallinity of titania coatings, and TiO_2 and silver modified TiO_2 powders was analysed using an X-ray diffractometer (Philips PANalytical X'pert Pro, Cu-K_α radiation). Powder samples were prepared in order to model the investigated TiO_2 and silver modified TiO_2 coatings: precursor sols (used in the preparation of TiO_2 and TiO_2/Ag coatings) were dried for 24 h until they formed a gel, then different heat-treatments were carried out. TiO_2 powders (heat-treated at 450 °C, 30 min) were impregnated in 0.03 M and 1 M $AgNO_3$ solution, filtered and dried, then heat-treated the same way as the respective coating samples after impregnation. From the XRD pattern the average crystallite sizes were determined from the highest intensity peak (corresponding to anatase (101) plane), using Scherrer's equation [34].

Transmission electron microscopy (TEM) and high-resolution transmission electron microscopy (HR-TEM) cross-sectional images of TiO_2 and TiO_2-Ag(1M) coatings on Si substrates were taken by a JEOL 3010 HRTEM (300 kV) with a point resolution of 0.17 nm). The microscope was equipped with a Tridiem GATAN Image Filter, making possible energy filtered TEM imaging, electron energy loss spectrum (EELS) measurements.

Wettability measurements of the samples were carried out using a drop shape analyser (DSA30, KRÜSS GmbH) device. Contact angles of distilled water were measured on TiO_2 coatings prepared on SiO_2 coated glass and on bare glass substrates. Advancing and receding contact angles were measured with the sessile drop method and the drop-build-up technique. The samples were placed in a closed chamber, where the relative humidity was kept above 90%, the temperature was 25 °C, and the following procedure was repeated three times on each sample: a water droplet of 10 µl was placed on the sample surface to measure the advancing contact angles, then 5 µl of water was removed to measure the receding angle. Contact angle hysteresis (H) was calculated as the difference of advancing (Θ_A) and receding (Θ_R) contact angles, and the Young's contact angle (Θ_{Young}) was calculated using the Wolfram-Faust equation [35]: $\Theta_{Young} = \arccos((\cos \Theta_A + \cos \Theta_R)/2)$. The photoinduced surface wettability conversion of the samples was studied by placing the samples under visible and UV light sources. The UV lamp was a Phillips CLEO UV-A light source (HPA 400 S, 400 W), with an emittance maximum in UV of 365 nm. The light arrived perpendicularly at the surface of the samples from a distance of 30 cm and intensity of 47.1 mW cm^{-2}. Two 57 W LED lamps (GE 93845, emission maximum at 600 nm) were used as visible light source, with a distance of 18 cm and intensity of 0.47 mW cm^{-2}.

Methyl orange dye, an anionic dye often used for the characterization of photocatalysts [36,37], was used as model pollutant in the photocatalysis tests: No methyl orange adsorption from their aqueous solution could be detected on the TiO_2 coating surface in preliminary experiments. 10^{-5} M methyl orange aqueous solutions were prepared using distilled water. The coatings were placed in glass crystallizing dishes, each containing 25 mL dye solution and irradiated with a UV lamp (the parameters of the UV irradiation were the same as described for the wettability measurements). Water bath and ventilation was used to counteract the heat generated by the high intensity UV lamp. The solution was mixed during the 4 × 1 h of UV irradiation. Before the measurement, and after each hour under UV light the absorption spectra of the dye solutions were measured in a quartz cuvette in the wavelength range of 350-600 nm, using distilled water as reference (otherwise using the same parameters as described above). In the repeated measurements, 4 × 4 h UV irradiation was repeated on TiO_2, TiO_2-Ag(0.03M), TiO_2-Ag(1M) and TiO_2/Ag coatings prepared only on one side of the glass substrate, using new dye solutions for each time. The samples were placed with the coated side upwards under the UV lamp. All photocatalysis test results were averaged from data measured on at least 3 identical samples in each case.

ACKNOWLEDGMENTS

The authors thank J. Sinclaire-Krasznai, P. Gömbös and E. Hild for their help. This work was supported by the Ministry of Human Capacities (BME FIKP-NAT); the National Research Development and Innovation Office (TNN-123631, K-128266); and the TÁMOP 4.2.1/B-09/1/KMR-2010-0002 (BME R + D + I project). Emőke Albert's research work was supported by the European Union and the State of Hungary, co-financed by the European Social Fund (TÁMOP-4.2.4.A/2-11/1-2012-0001).

REFERENCES

1. T. Ochiai; A. Fujishima; *J. Photochem. Photobiol. C Photochem. Rev.,* **2012**, *13*, 247–262.
2. M. Kapilashrami; Y. Zhang; Y.S. Liu; A. Hagfeldt; J. Guo; *Chem. Rev.,* **2014**, *114* (19), 9662–9707.
3. K. Nakata; A. Fujishima; *J. Photochem. Photobiol. C Photochem. Rev.* **2012**, *13* (3), 169–189.
4. C. Byrne; G. Subramanian; S.C. Pillai; *J. Environ. Chem. Eng.* **2018**, *6* (3), 3531–3555.
5. P. Hegedus; E. Szabó-Bárdos; O. Horváth; K. Horváth; P. Hajós; *Materials (Basel).* **2015**, *8* (1), 231–250.
6. M. Patil; S. Shaikh; I. Ganesh; *Curr. Nanosci.* **2015**, *11* (3), 271–285.
7. V.A. Ganesh; H.K. Raut; A.S. Nair; S. Ramakrishna; *J. Mater. Chem.* **2011**, *21* (41), 16304–16322.
8. R. Wang; K. Hashimoto; A. Fujishima; M. Chikuni; E. Kojima; A. Kitamura; M. Shimohigoshi; T. Watanabe; *Nature* **1997**, *338*, 431–432.
9. R.-D. Sun; A. Nakajima; A. Fujishima; T. Watanabe; K. Hashimoto; *J. Phys. Chem. B* **2002**, *105* (10), 1984–1990.
10. M. Miyauchi; N. Kieda; S. Hishita; T. Mitsuhashi; A. Nakajima; T. Watanabe; K. Hashimoto; *Surf. Sci.* **2002**, *511* (1–3), 401–407.
11. J. Schneider; M. Matsuoka; M. Takeuchi; J. Zhang; Y. Horiuchi; M. Anpo; D.W. Bahnemann; *Chem. Rev.* **2014**, *114* (19), 9919–9986.
12. S.G. Kumar; L.G. Devi; *J. Phys. Chem. A*, **2011**, *115*, 13211–13241.
13. J.G. McEvoy; Z. Zhang; *J. Photochem. Photobiol. C Photochem. Rev.* **2014**, *19* (1), 62–75.
14. E. Albert; P.A. Albouy; A. Ayral; P. Basa; G. Csík; N. Nagy; S. Roualdès; V. Rouessac; G. Sáfrán; Á. Suhajda; Z. Zolnai; Z. Hórvölgyi; *RSC Adv.* **2015**, *5* (73), 59070–59081.
15. S.P. Tallósy; L. Janovák; E. Nagy; Á. Deák; Á. Juhász; E. Csapó; N. Buzás; I. Dékány; *Appl. Surf. Sci.* **2016**, *371*, 139–150.

16. J.M. Herrmann; H. Tahiri; Y. Ait-Ichou; G. Lassaletta; A.R. González-Elipe; A. Fernandez; *Appl. Catal. B Environ.* **1997**, *13* (3–4), 219–228.
17. K. Awazu; M. Fujimaki; C. Rockstuhl; J. Tominaga; H. Murakami; Y. Ohki; N. Yoshida; T. Watanabe; *J. Am. Chem. Soc.* **2008**, *130* (5), 1676–1680.
18. K. Page; R.G. Palgrave; I.P. Parkin; M. Wilson; S.L.P. Savin; A.V. Chadwick; *J. Mater. Chem.* **2007**, *17* (1), 95–104.
19. W. Li; Z. Wu; J. Wang; A.A. Elzatahry; D. Zhao; *Chem. Mater.* **2014**, *26*, 287–298.
20. G. Zhao; H. Kozuka; T. Yoko; *Thin Solid Films* **1996**, *277* (1–2), 147–154.
21. M. Epifani; C. Giannini; L. Tapfer; L. Vasanelli; *J. Am. Ceram. Soc* **2000**, *83* (10), 2385–2393.
22. E. Traversa; M.L. Vona; D.I. Vona; P. Nunziante; S. Licoccia; T. Sasaki; N. Koshizaki; *J. Sol-Gel Sci. Technol.,* **2000**, *19*, 733–736.
23. I.M. Arabatzis; T. Stergiopoulos; M.C. Bernard; D. Labou; S.G. Neophytides; P. Falaras; *Appl. Catal. B Environ.* **2003**, *42* (2), 187–201.
24. P. Falaras; I.M. Arabatzis; T. Stergiopoulos; M.C. Bernard; *Int. J. Photoenergy* **2003**, *5* (3), 123–130.
25. L. Mai; D. Wang; S. Zhang; Y. Xie; C. Huang; Z. Zhang; *Appl. Surf. Sci.* **2010**, *257* (3), 974–978.
26. P. Novotna; J. Krysa; J. Maixner; P. Kluson; P. Novak; *Surf. Coatings Technol.* **2010**, *204* (16–17), 2570–2575.
27. M.M. Viana; N.D.S. Mohallem; D.R. Miquita; K. Balzuweit; E. Silva-Pinto; *Appl. Surf. Sci.* **2013**, *265*, 130–136.
28. C. Su; B.Y. Hong; C.M. Tseng; *Catal. Today* **2004**, *96* (3), 119–126.
29. J. Yu; J. Xiong; B. Cheng; S. Liu; *Appl. Catal. B Environ.* **2005**, *60* (3–4), 211–221.
30. D. Zhu; Z.A. Schelly; *Langmuir* **1992**, *8* (1), 48–50.
31. B. Tegze; E. Albert; B. Fodor; G. Sáfrán; Z. Hórvölgyi; *Dye. Pigment.* **2019**, *167*, 109–119.
32. E. Hild; A. Deák; L. Naszályi; Ö. Sepsi; N. Ábrahám; Z. Hórvölgyi; *J. Opt. A Pure Appl. Opt.* **2007**, *9* (10), 920–930.
33. W. Heller; *J. Phys. Chem.* **1965**, *69* (4), 1123–1129.
34. B.D. Cullity; *Elements of X-ray diffraction*, Addison-Wesley, London, **1956**, pp. 99.
35. E. Wolfram; R. Faust; *Wetting, Spreading Adhes.* **1978**, 213–222.
36. U.G. Akpan; B.H. Hameed; *J. Hazard. Mater.* **2009**, *170* (2–3), 520–529.
37. I.K. Konstantinou; T.A. Albanis; *Appl. Catal. B Environ.* **2004**, *49* (1), 1–14.